Automatic Localization of Curvilinear Object in 3D Ultrasound Images

Barva M.[a], Kybic J.[a], Mari J-M.[b], Cachard C.[b] and Hlaváč V.[a]

[a]Center for Machine Perception, CTU Prague, Prague, Czech Republic;
[b]CREATIS, CNRS, UMR 5515 U 630 INSERM, Lyon, France

ABSTRACT

Utilization of tools during surgical interventions sets the problem of their accurate localization within biological tissue. The ultrasound imaging represents an inexpensive and a flexible approach for a real-time image acquisition of tissue structure with metal instruments. There are several difficulties involving processing of ultrasound images: Their noisy nature makes the localization task difficult; the objects appear irregular and incomplete. Our task is to determine the position of a curvilinear electrode in biological tissue from a three-dimensional ultrasound image. Initially, the data are segmented by thresholding and processed with the randomized version of the RANSAC (R-RANSAC) algorithm. The curvilinear electrode is modeled by a three-dimensional cubic curve. Its shape is subject to check using a curvature measure in the hypothesis evaluation step of the R-RANSAC algorithm. Subsequently, we perform the least squares curve fitting to the data that have been marked by the R-RANSAC as the ones corresponding to the sought object. The position estimation is optimal with respect to the mean square criterion. Finally, the localization of the electrode tips is carried out by a hypothesis testing on the distances between projections of inliers on the estimated curve. The algorithm has been tested on real three-dimensional ultrasound images of a tissue mimicking phantom with a curvilinear object. From the results, we conclude that the method is very stable even if the data contain high percentage of outliers. The computational cost of the algorithm shows the possibility of real-time data processing.

Keywords: 3D ultrasound, image-guidance, needle, electrode, localization, curved, RANSAC

1. INTRODUCTION

The information about the position of small surgical instruments in human body is vital in many interventional procedures such as neuro-surgery, cardiac surgery, prostate therapy and breast biopsy. Although magnetic resonance[1] and computed tomography[2] have been used in tool guidance, the 3D ultrasound imaging is superior, permitting an inexpensive, flexible and fast acquisition of images that can serve for automatic object localization in biological tissue.[3]

An example of ultrasound data is in Figure 1. It depicts a three-dimensional ultrasound image of a biological tissue mimicking phantom with a metal electrode inside. The acoustical properties of a metal electrode are very different from the ones of biological tissue. The electrode appears in an ultrasound image as a region of higher brightness compared to the background. This is shown in Figure 1, where the electrode is marked with arrows. The electrode is very thin (in medical application less then one millimetre in diameter). It is therefore very likely to curve slightly as it penetrates the tissue. The goal of the proposed algorithm is to localize it, that is to say to estimate its position with respect to a given system of coordinates. This task can be interpreted as a curvilinear object localization in three-dimensional image data. Nevertheless, the nature of ultrasound image makes the localization difficult. Low dynamic range, speckle, distorted and missing parts of objects are some of the problems frequently encountered in ultrasound images. Several papers treating object localization in three-dimensional ultrasound images have been published.[4–6] They are either overly complex, which results in high computational cost inhibiting real-time processing, or they are restrictive in terms of the object shape that can be localized. This paper presents a novel image processing algorithm that overcomes such limitations and makes a near real-time object localization possible.

Further author information: (Send correspondence to Barva M.)
E-mail: barvam1@fel.cvut.cz, Telephone: +420 2 2435 5725

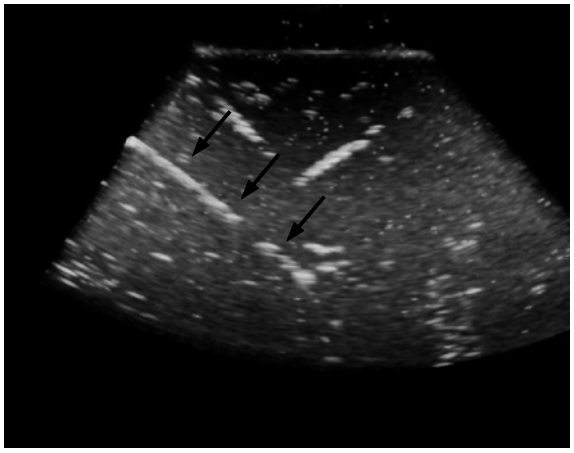

Figure 1. Three-dimensional ultrasound image of a metal electrode (marked with arrows) in a phantom mimicking acoustical properties of biological tissue.

The contribution of this paper can be summarized into following points. We developed of a novel method for stable and fast localization of curvilinear objects in three-dimensional ultrasound images. The curve localization in three-dimensional space is based on the randomized RANSAC with a curvature measure. The tips of the electrode are statistically localized. This allows their robust localization even if a small part is missing.

The structure of this paper is as follows. First, in Section 2, the proposed method and its steps are presented in details. In Section 3 experiments and their results are shown. The paper is concluded in Section 4 and plans for future work are discussed.

2. PROPOSED METHOD

This section of the paper contains a description of the developed method. Each step of the method is applied to the image in Figure 1 to show its particular effect. As we have already mentioned, Figure 1 represents a three-dimensional image reconstructed from ultrasound data. Mathematically, the image can be described by an image function

$$I : A \rightarrow B \tag{1}$$

where A is a set of voxels coordinates and B is a set of non-negative voxel values.

Throughout this section, we will use the following notation. By the term *object voxels* we understand the voxels that correspond to the object to localize (the metal electrode). Similarly, *background voxels* denotes voxels corresponding to non-object voxels (biological tissue, air, liquid, etc.). Moreover, we shall refer to selected object, resp. to background voxels as *inliers*, resp. *outliers*.

2.1. Brief description of the method

Initially, the voxel values are segmented by thresholding. The choice of the threshold value is not critical, due to a large difference between the value of voxels corresponding to the metal electrode and soft tissue. The speckle and other phenomenons cause that the result of thresholding contains a large number of false positives. In order to discriminate them from the electrode (inliers), we exploit the randomized version[7] of the RANSAC algorithm.[8] This ensures the robustness of the method even if the data contain a significant portion of noise. The curvilinear electrode is modeled by a three-dimensional cubic curve. This represents a good trade-off between the range of shapes that can be modeled, and the extent of undesired ripples typical for higher-degree polynomials. To further control the curvature oscillations, a curvature measure is calculated in the hypothesis evaluation step of the R-RANSAC algorithm. Next, we perform the least squares curve fitting on the voxels that have been marked by the R-RANSAC as inliers. If the inlier noise has a normal distribution, the error of position estimation will be

minimal with respect to the least mean squares criterion. Lastly, the position of the electrode tips is localized by hypothesis testing. We assume that the length of the gaps between projections of inliers on the estimated curve has a known probability distribution. The longest interval in which the gaps are below a statistically chosen threshold are marked as the electrode. This approach provides correct electrode endpoint localization even if a part of the electrode in the image is missing.

2.2. Image segmentation

In the first step, we segment the image by binarization with a constant threshold. This simple operation has two goals. First, we want to roughly distinguish between the object voxels (inliers) and background voxels (outliers). The second objective is to decrease the amount of data to process.

The threshold T is heuristically set to such a value that 10% of the voxels with the highest value in $I(A)$ are set to one, meanwhile the values of the rest of the voxels are set to zero. The use of binarization can be justified by the fact that in ultrasound data the object voxels have in general much greater values than background voxels. This follows from different acoustical properties of the metal electrode and biological tissue. Let's define a set of voxels $S = \{\vec{x} \,|\, I(\vec{x}) \geq T\}$ with the value greater or equal to T. The result of the segmentation is in Figure 2.

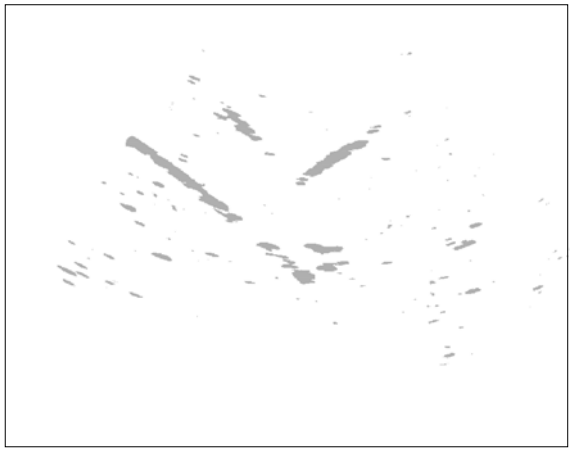

Figure 2. The result of segmentation of the image in Figure 1 by thresholding. Only the voxels from the set S are shown.

2.3. Object localization

The result of the segmentation contains a large number false positives, see Figure 2. Therefore, we employed a second classification mechanism that reclassifies each voxel from the set S. It is based on the model fitting approach: The object is described by a mathematical model and the model is fitted to selected points from the set S. Its parameters are calculated so that it matches the selected points of S. Finally, voxels from the set S are classified as inliers if they are consistent with the estimated model, otherwise they are marked as outliers (see (4) for the definition of the point-model consistency).

2.3.1. Mathematical model of the object

The electrode appears in the ultrasound image as a cylinder with a curvilinear centerline. We model the centerline with a three-dimensional cubic curve with a parametrization l given by the formula

$$l : t \mapsto (x(t), y(y), z(t)), \tag{2}$$

where $t \in [t_0, t_1]$ and

$$\begin{aligned} x(t) &= a_0 + a_1 t + a_2 t^2 + a_3 t^3 \\ y(t) &= b_0 + b_1 t + b_2 t^2 + b_3 t^3 \\ z(t) &= c_0 + c_1 t + c_2 t^2 + c_3 t^3 \end{aligned} \tag{3}$$

The degree of the curve was chosen as a trade off between the range of shapes that can be modeled and the extent of undesired ripples typical for higher degree polynomials. The model is determined by a parameter vector $\Theta = (a_0, a_1, a_2, a_3, b_0, b_1, b_2, b_3, c_0, c_1, c_2, c_3)$.

2.3.2. Estimation of the vector of parameters Θ

The parameter vector Θ is estimated by a R-RANSAC,[7] a randomized version of the RANSAC*[8] algorithm. It can treat data sets containing a significant proportion of outliers. Repeatedly, random subsets of the input data are selected. Model is then fitted to each sample subset. The subsets are as small as possible wile permitting to determine the model parameters. In the second step, the quality of the fit is evaluated on the complete data set. The process is terminated when the likelihood of finding a better model becomes low. In the R-RANSAC, the hypothesis evaluation step is modified in the sense that it is a two-stage procedure. First, a statistical test[7] is performed on d randomly selected data points (according to,[7] we set d to one). The final evaluation on all data points is carried out only if the test in the first stage is passed. This accelerates the estimation while preserving its robustness.

Implementation This paragraph summarizes the estimation of the parameter vector Θ by the R-RANSAC algorithm.

`Input:` `Set` S.

`Output:` `Parameter vector` $\hat{\Theta}_R$ `estimated by the R-RANSAC algorithm.`

`Iterations:` $k := 0$. `Repeat steps 1-4 until` $P\{\text{better solution exists}\} < \eta$.

The number of iterations is set to such a value that the probability of the event "better-than-currently-best estimated model is missed" is less than η (in our implementation $\eta = 0.05$ requires 500 iterations). See the reference[7] for details on how to set the number of iterations.

1. $k := k + 1$.
2. `Hypothesis generation`
   (a) `Select a random subset` $S_k \subset S$, $|S_k| = 4$.
   (b) `Compute` Θ_k `from` $f(S_k)$.
   $|S_k|$ is 4, since the number of unknowns in (3) is 12 and each point from S has three coordinates. These 12 linear equations with 12 unknowns define a function $f(S_k) = \Theta_k$ permitting to fit the model described by Θ_k to S_k.
3. `Preliminary test`
   (a) `Test consistency of one randomly selected data point with the model described by the vector` Θ_k.
   This test is passed if a randomly selected point from the set S is consistent with the estimated model (the consistency is defined by (4)).
   (b) `Go to 4, if the test is passed, otherwise return to 1.`

*Random SAmple Consensus

4. `Model quality evaluation`

   (a) `Compute the number of consistent points` $N_C(\Theta_k)$ `and an approximated curvature` $\kappa(\Theta_k)$`.`
   We say that a point $\vec{x}$ is consistent with a curve $l_\Theta(t)$ if

$$d(l_\Theta(t), \vec{x}) = \min_{t \in \mathbb{R}} \|l_\Theta(t) - \vec{x}\|_2 \leq \varepsilon, \tag{4}$$

   where ε is an estimated electrode diameter. Let $C_\Theta = \{\vec{x} \in S \,|\, d(l_\Theta(t), \vec{x}) \leq \varepsilon\}$ and $N_C(\Theta) = |C_\Theta|$. By taking into account the value $\kappa(\Theta_k)$, we give preference to curves that are not very curved. Figure 3 compares the result of vector Θ estimation with and without the curvature control.

   (b) `If` $N_C(\hat{\Theta}_R) < N_C(\Theta_k)$ `and` $\kappa(\hat{\Theta}_R) > \kappa(\Theta_k)$`, then` $\hat{\Theta}_R := \Theta_k$`.`
   There must be an improvement in both criteria, $N_C(\Theta_k)$ and $\kappa(\Theta_k)$ for a new model to be accepted.

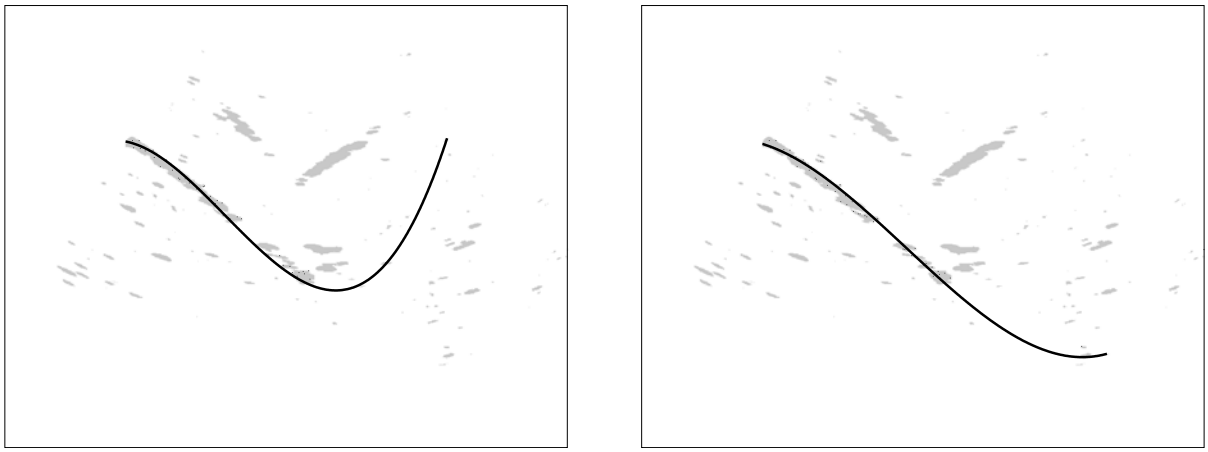

Figure 3. The effect of curvature measure in the model evaluation step. Darker voxels are consistent with the curve; a) without curvature measure, b) with curvature measure.

2.4. Improvement in localization accuracy

Although the R-RANSAC algorithm gives stable results, the estimated model is not optimal, because the estimate is based only on four randomly selected points.

Let $C_{\hat{\Theta}_R}$ be the set of points that are consistent with the curve $l_{\hat{\Theta}_R}(t)$. Based on the set of inliers $C_{\hat{\Theta}_R}$ from R-RANSAC, we shall find a solution $\hat{\Theta}_J$ that minimizes the criterion

$$J(l_\Theta(t), C) = \sum_{\forall \vec{x} \in C} d(l_\Theta(t), \vec{x}) \tag{5}$$

The procedure to minimize (5) is the least mean square curve fitting. Upon the assumption that the inlier distance $d(l_{\hat{\Theta}_J}(t), \vec{x})$ from the centerline has a normal distribution, the vector $\hat{\Theta}_J = \arg\min_\Theta J(l_\Theta(t), C_{\hat{\Theta}_R})$ is an optimal estimate of the parameter vector Θ in the maximum likelihood sense.

The result of the minimization is shown in Figure 4. The left hand side image depicts the curve $l_{\hat{\Theta}_R}(t)$, whereas on the right hand side there is the curve $l_{\hat{\Theta}_J}(t)$.

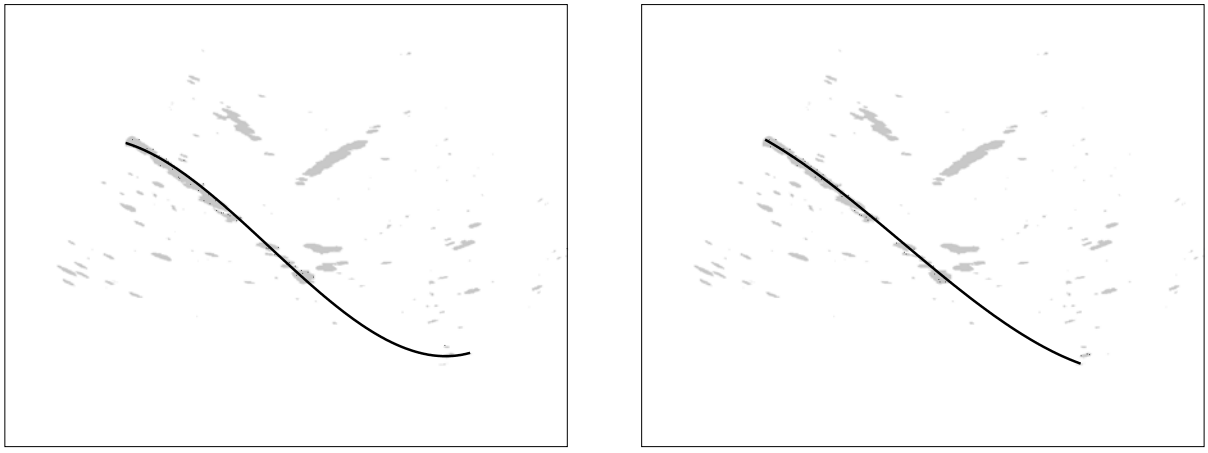

Figure 4. Improvement in object localization accuracy; a) curve with the parameter vector $\hat{\Theta}_R$, b) curve with the improved parameter vector $\hat{\Theta}_J$.

2.5. Endpoint localization

At this stage, we have the vector of parameters $\hat{\Theta}_J$ defining a cubic curve with the parametrization $l_{\hat{\Theta}_J}(t)$ that passes through the points from the set C. In the last step of the method, we localize two points on the curve corresponding to the electrode endpoints.

We propose a statistical based method to localize the endpoints. First, the points from the set C are orthogonally projected on the curve $l_{\hat{\Theta}_J}(t)$ to obtain a set of projections, $C^p = \{x_i^p\}$. Define $t_i \in \mathbb{R}$, such that the equality $l_{\hat{\Theta}_J}(t_i) = \vec{x}_i^p$ holds for each $i = 1, 2, \ldots, N = |C^p|$. Create a sequence $\{\vec{x}_1^p, \vec{x}_2^p, \ldots, \vec{x}_N^p\}$ such that $t_1 \leq t_2 \leq \cdots t_N$. We calculate the Euclidean distance d_i between the points $\vec{x}_{i-1}^p$ and $\vec{x}_i^p$, $d_i = \|\vec{x}_{i-1}^p - \vec{x}_i^p\|_2$; $\forall i = 1, 2, \ldots, N$. Figure 5 is a graphical representation of d_i as a function of index i. Let D be a vector $\{d_1, d_2, \ldots, d_N\}$

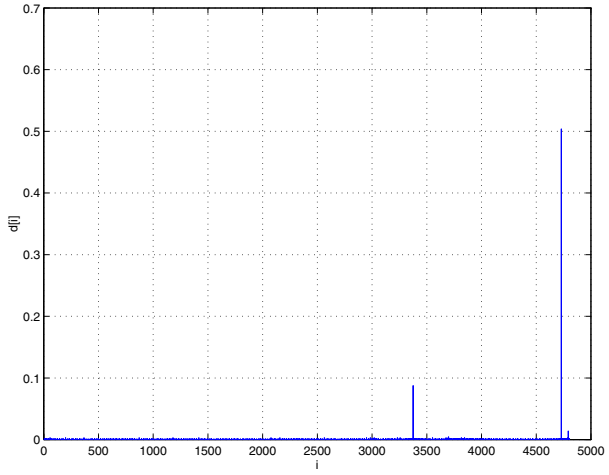

Figure 5. Graphical representation of distances d_i as a function of i.

The voxels along the curve $l_{\hat{\Theta}_R}(t)$ are contaminated with noise. Consequently, the distance d_i is a random variable X with some unknown probability distribution F. Then the vector $(d_1, d_2, \ldots, d_N)$ can be interpreted

as a random sample from the distribution F. As d_i represents a distance, a positive number, we assume X to have the log-normal distribution. Define a new random variable $Y = \ln X$. Then Y has the normal distribution $G = N(\mu, \sigma^2)$. The parameters μ and σ^2 are estimated from the sample mean and sample variance

$$\hat{\mu} = \frac{1}{|K|} \sum_{\forall d_i \in K} \ln d_i; \qquad \hat{\sigma}^2 = \frac{1}{|K| - 1} \sum_{\forall d_i \in K} (\ln d_i - \hat{\sigma})^2, \tag{6}$$

where $K \subset D$ is a subset of sample points lying in the interquartile range (25%-75%), that is, the points that are assumed to lie on the electrode.

Given the estimated probability density of the random variable Y, we can guess whether a pair of points $\vec{x}_{i-1}$, $\vec{x}_i$ lies within the object voxels. The classification is based on the interval confidence (at the confidence level 5%) applied to the random variable Y. We assume that the pair x_{i-1}, x_i is in the same compact region iff d_i is in the interval of confidence. The voxels lying inside the longest compact region are marked as object voxels. The final results of the algorithm is shown in Figure 6.

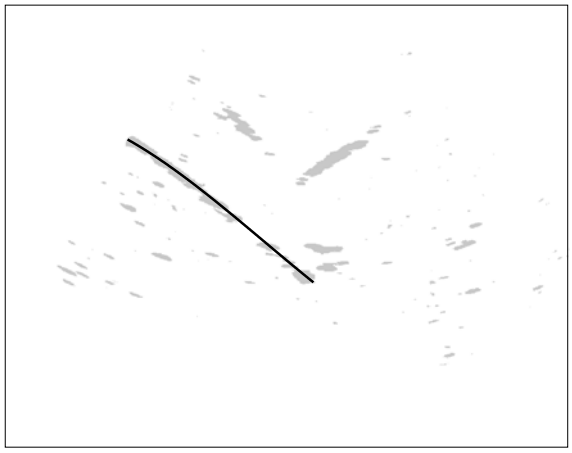

Figure 6. Final result of the algorithm. The localized curve is shown in black.

3. RESULTS

The functionality of the algorithm was verified on real ultrasound data acquired by the ultrasound scanner Kretz Voluson 530D. A metal electrode with diameter 0.5mm was inserted into a phantom mimicking acoustic properties of biological tissue. It was scanned by a three-dimensional ultrasound scanner equipped with a mechanically tilted transducer operating at central frequency 7.5MHz. The size of the volumetric data was 500x450x90 voxels. Figure 7 shows an example of the localization. On the left, there is the original ultrasound image. The right-hand side image shows the localized electrode marked in black. Other experiments show that the localization is stable even if the input data is very noisy.

4. CONCLUSION

The three-dimensional ultrasound imaging plays a key role in many applications in image-guided surgery, biopsy, and therapy. Along with them, there is a need for image processing algorithms capable of automatic object localization. Due to the low quality of ultrasound data, this task is particularly challenging. In this paper we present a novel algorithm that makes possible the localization of curvilinear objects such as a bent metal electrode in biological tissue from an ultrasound image. It deals with the known problems encountered in ultrasound data. The results are stable even when the data contain high amount of noise. The least mean square fitting minimizes the mean square error of position estimation. Further, the method can handle also cases when a part of the

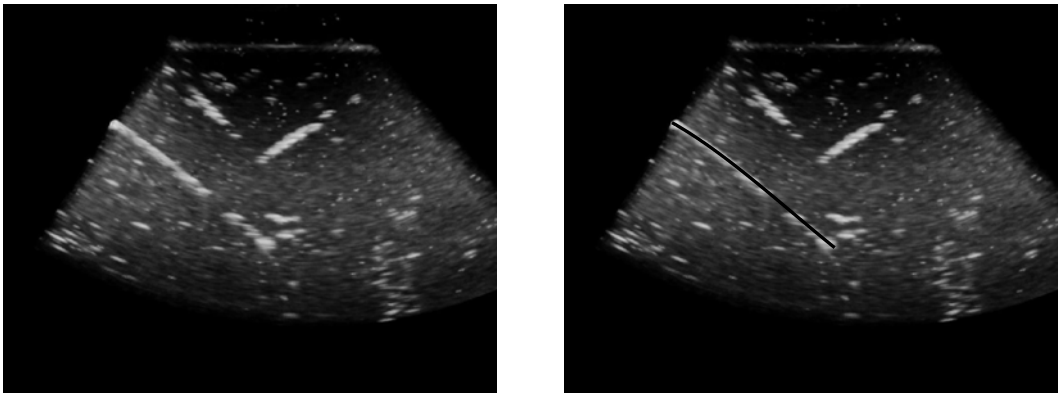

Figure 7. Three-dimensional ultrasound image of a metallic electrode in a phantom. The size is 500x400x90 voxels; a) original image with a partially missing electrode, b) result of the algorithm (localized electrode is marked as a black line-segment).

electrode in the data is missing. Finally, its real-time implementation is feasible. The forthcoming work will focus on algorithm acceleration.

ACKNOWLEDGMENTS

The 1st author was supported by The Grant Agency of the Czech Academy of Sciences under project 1ET101050403 (Artificial Intelligence Methods in Diagnostics from Medical Images) and by the French Embassy under the project of doctoral studies with co-supervision. The 2nd author was supported by the The Czech Ministry of Education under project MSM6840770012 (Transdisciplinary Biomedical Engineering Research II).

REFERENCES

1. P. M. Black, T. Moriarty, E. Alexander, P. Stieg, and E. J. Woodard, "Development and implementation of intraoperative magnetic resonance imaging and its neurosurgical applications," *Neurosurgery* **41**(831–845), 1997.
2. G. D. Schweiger, V. Y. Yip, and B. P. Brown, "Ct fluoroscopic guidance for percutaneous needle placement into abdominopelvic lesions with difficult access routes," *Abdominal Imaging* **25**, November 2000.
3. A. Fenster, B. D. Donal, and H. N. Cardinal, "Three-dimensional ultrasound imaging," *Physics in Medicine and Biology* **46**, May 2001.
4. M. Ding, H. N. Cardinal, W. Guan, and A. Fenster, "Automatic needle segmentation in 3d ultrasound images," in *Proceedings of SPIE*, **4681**, pp. 65–76, International Society for Optical Engineering, May 2002.
5. P. M. Novotny, J. W. Cannon, and R. H. Howe, "Tool localization in 3D ultrasound images," in *Proceedings of Medical Image Computing and Computer-Assisted Intervention*, **2879**, pp. 969–970, Springer-Verlang, Berlin, 2003.
6. K. J. Draper, C. C. Blake, D. B. Gowman, L. nad Downey, and A. Fenster, "An algorithm for automatic needle localization in ultrasound-guided breast biopsies," *Medical Physics* **27**, pp. 1971–9, 2000.
7. O. Chum and J. Matas, "Randomized RANSAC with t(d,d) test.," in *Proceedings of the British Machine Vision Conference, Cardiff, UK*, pp. 448–457, 2002.
8. M. A. Fischler and R. C. Bolles, "Random sample consensus: A paradigm for model fitting with applications to image analysis and automated cartography," *CACM* **24**, pp. 381–395, June 1981.